Preparation and evaluation of chitosan-hydrophobic silica composite microspheres: Role of hydrophobic silica in modifying their properties

B. P. Da Costa Neto, A.L.M.L. da Mata, Milene V. Lopes, B. Rossi-Bergmann, Maria-Inês Ré

Preparation and evaluation of chitosan–hydrophobic silica composite microspheres: Role of hydrophobic silica in modifying their properties

B.P. da Costa Neto [c], A.L.M.L. da Mata [c], Milene V. Lopes [d], B. Rossi-Bergmann [d], M.I. Ré [a,b,*]

[a] Université de Toulouse, Mines Albi, CNRS, Centre RAPSODEE, Campus Jarlard, F 81013 Albi CT cedex 09, France
[b] Laboratory of Chemical Processes and Particle Technology, IPT, Institute for Technological Research, São Paulo, Brazil
[c] Chemical Engineering Department, Federal University of Rio Grande do Norte (UFRN), Natal, Rio Grande do Norte, Brazil
[d] Institute of Biophysics Carlos Chagas Filho, Federal University of Rio de Janeiro (UFRJ), Rio de Janeiro, Brazil

A B S T R A C T

Biodegradable microspheres used as controlled release systems are important in pharmaceutics. Chitosan biopolymer represents an attractive alternative to other biomaterials because of its significant physicochemical and biological behaviors. Chitosan microspheres are expected to become promising carrier systems for drug and vaccine delivery, especially via oral, mucosal and transdermal routes. Controlling the swelling rate and swelling capacity of the hydrogel and improving the fragile nature of microspheres under acidic conditions are the key challenges that need to be overcome to allow the use of chitosan microspheres for controlled or sustained release specially via these non-invasive administration routes.

There have been many studies on the modification of chitosan microsphere structures with cross-linkers, blends with various kinds of polymers and new organic–inorganic hybrid systems in order to obtain some improved properties. In this work, microspheres composed of chitosan and nanosized hydrophobic silica commercialized under the name Aerosil R972 were generated by a method consisting of two steps: first, preparation of a macroscopically homogeneous chitosan–hydrophobic silica dispersion by an optimized procedure, and then drying. Spray drying was the technique used here. FTIR spectroscopy, X-ray powder diffraction, differential scanning calorimetry, thermal gravimetric analysis, Scanning Electron Microscopy (SEM) and high resolution Transmission Electron Microscopy (TEM) were used to characterize the microspheres, besides acid stability, moisture sorption capacity, release properties and biological assays.

The chitosan–hydrophobic silica composite microspheres showed improved thermal degradation, lower water affinity, better acid stability and ability to retard rifampicin (drug model) release under simulated gastric conditions. In vitro biocompatibility studies indicated low cytotoxicity and low capacity to activate cell production of the pro-inflammatory mediator nitric oxide, encouraging further studies on the use of the new chitosan–hydrophobic silica composite microspheres as drug carrier systems via oral or nasal routes.

Keywords:
Chitosan
Spray drying
Nanocomposite
Drug delivery

1. Introduction

Chitosan is a biopolymer derived from chitin, a natural polysaccharide usually obtained from carapaces of marine crustaceans such as crabs and shrimps [1]. Due to its natural origin, chitosan cannot be defined as a unique chemical structure, but as a family of polymers of different molecular weights and degrees of deacetylation, defined in terms of the percentage of primary amino groups in the polymer backbone [2].

Chitosan has many physicochemical (reactive hydroxyl and amino groups, high positive charge in acidic conditions, good film formation) and biological (biocompatible, biodegradable, lack of toxicity, antimicrobial effects, mucoadhesive character) properties, that make it an attractive material for use as a new functional material of high potential in fields as different as biomedical [3–5], food [6–9], water treatment [5,10–12], and agricultural [9,12,13], among others. Chitosan has, for example, the ability to bind to particular materials including proteins, metal ions, and even tumor cells. Moreover, chitosan can be incorporated into hydrogels and microspheres which demonstrate large potential in delivery systems for drugs via oral, nasal or transdermal routes [14–18].

Chitosan has many advantages, particularly for developing nano/microspheres as carrier systems. These include its ability to control the release of active agents and to avoid the use of hazardous organic solvents while fabricating particulate systems, since it is soluble in aqueous acidic solution. However, the stability of the chitosan microspheres under different physiological conditions is a prerequisite for their successful application. For example, microspheres intended for nasal administration have to be optimized in terms of particle size and surface charges necessary to induce mucoadhesiveness. Chitosan has been

* Corresponding author at: Université de Toulouse, Mines Albi, CNRS, Centre RAPSODEE, Campus Jarlard, F 81013 Albi CT cedex 09, France. Tel.: +33 5 6349 3299; fax: +33 56 349 3025.
E-mail address: maria-ines.re@mines-albi.fr (M.I. Ré).

shown to possess mucoadhesive properties owing to the electrostatic interaction between its positive charges and negatively charged mucosal surfaces. However, chitosan microspheres absorb water, swell and become too fragile after being swollen, losing their rigidity and shape, which can clog the nostrils and hampers intranasal delivery. Another example is the considerable limitation of chitosan microspheres as sustained release carrier systems for oral administration. Chitosan rapidly adsorbs water, swells and dissolves under gastric conditions, leading to fast drug release.

In order to overcome these problems, it is possible to modify the chitosan structure by introducing cross-linking structure, blending chitosan with synthetic polymers such as poly(vinyl alcohol) (PVA) [19], and developing organic–inorganic hybrid membranes [20].

Cross-linking is a common way to improve the controlled-release properties and mechanical strength by introducing a three-dimensional network structure [21]. Consequently, the motion of solutes across cross-linked polymer membranes can be controlled by precisely controlling this network structure. The available amino and hydroxyl groups on chitosan are active sites capable of forming a number of linkages. To date, the most common cross-linkers used involving bonds with chitosan amine groups are aldehydes, such as glutaraldehyde [22–24], formaldehyde [25,26] or glyoxal [27,28]. Epichlorohydrin, a bifunctional molecule which contains two functional groups, is another cross-linker reagent highly reactive with the hydroxyl groups of chitosan [29,30].

Cross-linked chitosan networks are highly useful in the pharmaceutical field for the formulation of various novel drug delivery systems like microspheres, nanospheres and films/membranes. However, acceptance of such cross-linked products depends upon the amount of cross-linking agent present in the final products. In that sense, the toxicity of aldehydes has enormously limited the exploitation of the cross-linked chitosan microparticles in the pharmaceutical field [31,32]. To overcome toxicity, Ré and co-workers have also long been studying the potential use of d,l-glyceraldehyde as a biocompatible cross-linking agent, since it is present in the human organism as a metabolic product of fructose. The morphology, particle size, surface charge and water-uptake capacity properties of the cross-linked chitosan microspheres have been characterized and published [33,34].

In another way, chitosan–clay nanocomposites have been synthesized as coating materials for tablets to retard acid swelling and improvement of film stability in gastric fluid. Clays are composed of silicate layers. The silicate layers can be separated and form three-dimensional structures when they are hydrated in water. They have negative charge and can interact with chitosan. It was found that chitosan reacts with several types of clays such as montmorillonite [35–38], magadiite [39], rectorite [20] or magnesium aluminum silicate [40] for modified-release tablets. Montmorillonite chitosan nanocomposites have been proposed as new drug delivery for oral administration combining mucoadhesive properties with low solubility in acidic environment for modified drug delivery formulations [37].

Silica has already been combined with chitosan to synthesize silica–chitosan hybrid materials by sol–gel process under acid conditions in various structures such as hierarchical porous materials and composite membranes [16,40–43]. We proposed here an alternative way to control chitosan microsphere properties such as moisture sorption capacity, acid stability, surface charge and release properties by combining chitosan with nanosized organic silica oxide named Aerosil R972 into chitosan composite microspheres. The objective of this work was to produce chitosan–Aerosil R972 composite microspheres by spray drying and to examine the role of the nanosized modified silica in modifying their properties.

2. Materials

Low molecular weight chitosan (75–85% deacetylated chitosan) was purchased from Sigma-Aldrich (St. Louis, MO, USA). Hydrophobic silica named Aerosil R972 (primary particle size of 16 nm, specific surface area of 110 ± 20 $m^2\ g^{-1}$) was supplied by Degussa-Huls Corporation, Brazil. Analytical grades of absolute ethanol, anhydrous acetic acid, dimethyl sulfoxide, hydrochloric acid and sodium hydroxide used in this study were provided by Synth (Brazil).

Cell culture reagents: Dulbecco Modified Minimum Essential Medium (DMEM) and heat inactivated fetal calf serum were obtained from Cultilab, Brazil; lipopolysaccharide, Triton X-100 and the Griess reagents were from Sigma Aldrich. The lactate dehydrogenase kit was purchased from Doles, Brazil. Rifampicin, $C_{43}H_{58}N_4O_{12}$ (structural formula given in Fig. 1), was used as drug model. The raw material (purity >99%) was obtained from Luohe Nanjiecun Pharmaceutical (Group Pharmacy China) and used without further purification.

3. Methods

3.1. Measurements of the contact angle of ethanol–water solutions on Aerosil R972

The first problem to be solved in this study was how to properly disperse a hydrophobic nanosized material like Aerosil R972 into an aqueous solution of chitosan. We proposed the introduction of ethanol in the mixture to facilitate the silica wetting and dispersion. To define the concentration values of ethanol/water mixtures to be used, the Aerosil R972 powder was pressed in tablets and the wetting of water/ethanol mixtures on the silica tablet surfaces was analyzed by the sessile drop method coupled with digital image analysis. Briefly, a liquid drop of water/ethanol mixture was gently deposited on the solid substrate and the profile of the drop was captured digitally by using an optical microscope.

3.2. Preparation of chitosan–Aerosil R972 microspheres

The chitosan solution (1 g) was prepared by dissolving the polymer in deionized water containing 3% w/v acetic acid (approximately 80 ml). The mixture was maintained under mechanical stirring for 30 min. After complete dissolution the pH was adjusted to 5.5–6.0 with a 0.5 M NaOH solution.

In order to facilitate the dispersion of the nanosized particles of Aerosil R972 in the aqueous chitosan solution, they were first wetted with absolute ethanol (approximately 25 ml). Next, the ethanolic dispersion was added to the chitosan solution under stirring (200 rpm) to give, after this dilution, a dispersion containing 20% w/w ethanol, able to ensure silica wetting in the hydroalcoholic dispersion. We then homogenized the dispersion in order to break potential particle aggregates, using a high-pressure homogenizer (model APV-2000, Stansted Fluid Power, APV, USA) operated at 800 bar for five homogenization cycles (15 min).

Chitosan–Aerosil R972 microspheres were then produced with the subsequent removal of the solvent of the homogenized suspensions.

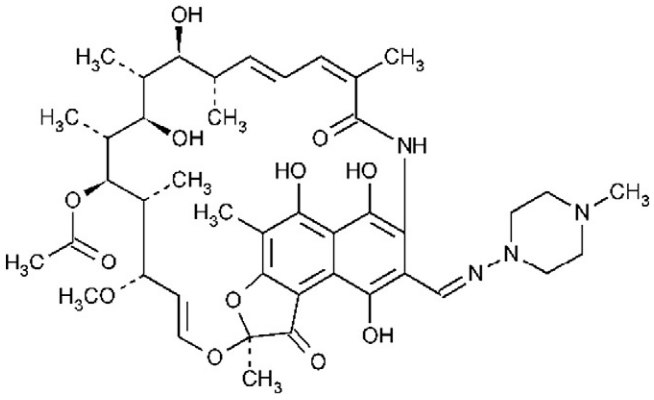

Fig. 1. Chemical structure of the drug model (rifampicin) used in this study.

They were spray dried with a 0.5 mm two-fluid pressurized atomizer at a feed rate of 3 ml min^{-1} in a Büchi-B190 spray dryer (Buchi Labortechnik AG, Flawil, Switzerland). The atomizing air flow rate was 600 NL/h. The inlet temperature was controlled at 120 ± 2 °C and the outlet temperature at 89 ± 3 °C. The experiments were made in triplicate.

Before spray drying, the viscosities of the hydroalcoholic dispersions were measured at 5 rpm and at 25 ± 0.2 °C with a Brookfield viscometer (DV-III Ultra). The viscometer was operated with spindle no. SC4-31. The viscosity values were analyzed with the Brookfield's Rheocalc software.

3.3. Characterization of chitosan–Aerosil R972 microspheres

3.3.1. Particle size, surface area, morphology and zeta potential

Particle size distributions were determined using a laser diffraction particle size analyzer in the polarization intensity differential scattering (PIDS) optical mode (Beckman Coulter, model LS 230, Miami, FL). Samples of spray dried powders were dispersed in mineral oil, until the required obscuration (about 40% PIDS) was achieved. Average particle size was expressed as the volume mean diameter ($D_{4,3}$). Polydispersity was given by a span index, which was calculated by $(D_{0.9} - D_{0.1}) / D_{0.5}$, where $D_{0.9}$, $D_{0.5}$ and $D_{0.1}$ are the particle diameters determined respectively at the 90th, 50th and 10th percentiles of undersized particles. The measurements were performed in triplicate.

The surface area was measured by the technique of Brunauer, Emmett and Teller (BET), using the equipment ASAP 2010, Micromeritics (USA). Microparticle samples were weighted (0.5 g) in glass tubes and pretreated to remove moisture in an oven with circulating air at 50 °C for approximately 12 h. In the range of validity of the BET isotherm, the specific area was calculated from the slope and intercept of the line formed by five points of measurement.

The particles were observed by Scanning Electron Microscopy (SEM) (JEOL JSM-6360LV, Japan) after Au coating and by Transmission Electron Microscopy (TEM) (Philips CM120 80 kV) after embedding the microspheres with Spur epoxy resin and microtome-sectioning for TEM analysis.

The zeta potential was measured by electrophoretic mobility using a DelsaNano C (Beckman Coulter, USA). All samples were dispersed in deionized water and the pH was adjusted (4.0 to 7.4) by adding HCl 0.5 M or NaOH 0.5 M. Each zeta potential value reported is an average of at least 10 measurements.

3.3.2. Structural characterization

The moisture content was measured by Karl Fisher titration in dry methanol using a DL38 titrator (Mettler-Toledo, Switzerland). Measurements were made in triplicate.

FTIR spectra were recorded on a Nicolet 6700 FTIR- spectrophotometer (Thermo Scientific, USA) using a KBr disk in the range of 4500–500 cm^{-1}, with 4 cm^{-1} resolution.

TG curves of samples were obtained by a TG-Mark Mettler Toledo, Model SDTA851. A standard sample holder of alumina ceramic (Al_2O_3) was used. The samples were weighed on a precision balance Mettler Toledo Brand, Model XS205. The analyzes were performed under an atmosphere of oxygen at a flow rate of 50 ml min^{-1}, from 0 to 800 °C at a heating rate of 10 °C min^{-1}. The inorganic content of the spray dried powders was determined by weighting the remaining ash after complete degradation of the samples at 800 °C.

The DSC thermograms of the samples were obtained by a Differential Scanning Calorimeter DSC822 (Mettler Toledo) using a standard aluminum sealed sample holder where the samples were weighed on a precision balance Mettler Toledo Brand, Model XS205. The analyses were performed under an atmosphere of oxygen at a flow rate of 50 ml min^{-1} in the temperature range of 20–450 °C at a heating rate of 10 °C min^{-1}.

For DRX analysis the samples were pressed in an aluminum sample holder and data were collected on an X-ray diffractometer Shimadzu, XRD 6000, CuKα radiation (λ = 1.5418 A), operating at 40 kV and 40 μA voltage and tube current, respectively. The scan was made over the range 2Θ from 5 to 40° with a step of 0.02° and 5 s/step. The results were obtained from XRD-6000 software programs.

3.3.3. Water sorption characteristics

Sorption profiles were determined using an automated water sorption analyzer (DVS-2, Surface measurement systems Ltd., London, UK). The DVS-2 measures the uptake and loss of vapor gravimetrically using a recording microbalance. The relative humidity around the sample was controlled by mixing saturated and dry carrier gas streams using mass flow controllers. The temperature was kept constant. Prior to being exposed to any water vapor the sample was dried at O% RH to remove any water present. Next, the sample was exposed to the desired relative humidity and the moisture uptake was measured. This was performed over a series of relative humidities at 25 °C. The amount of water adsorbed and/or desorbed was expressed as a percentage of the dry sample. More specifically, approximately 100 mg of sample was weighed into the sample pan of the DVS and subjected to two 0–90% relative humidity (RH) sorption cycles, over 10% RH increments. Equilibrium sorption at each humidity step was determined by a change in mass to time ratio of 0.007 dm/dt. Each sample was submitted to three sorption–desorption cycles.

3.3.4. Acid stability

The stability of the spray dried microspheres in 0.1 N HCl was determined by incubating 0.5% w/v suspension of the microspheres in 0.1 N HCl for 60 min and measuring the transmission of the samples at 500 nm (Spectrophotometer CINTRA 10E, GBC Melbourne, Australia) after they had been exposed to the acidic medium, as already reported [44,45].

3.3.5. Biological assays

3.3.5.1. Nitric oxide production by macrophages. Macrophages were obtained by the peritoneal lavage of BALB/c mice. Peritoneal cells were allowed to adhere to 96-well culture microplates (TPP) at 4×10^5 cells/well in 100 μl of DMEM medium. After 1 h at 37 °C and 5% CO_2, the non-adherent cells were removed and the adherent macrophages were cultured for a further 48 h in the presence or absence of increasing concentrations of spray dried microspheres in 200 μl of DMEM medium plus 10% heat inactivated fetal calf serum and 1% DMSO. For positive stimulation, cells were cultured with 1 μg ml^{-1} of lipopolysaccharide (LPS). Untreated cells were cultured in medium alone. At the end of incubation, the culture plates were centrifuged at 500 rpm during 5 min, and the nitric oxide production was indirectly determined in the cell culture supernatants by its nitrite oxidation product using the colorimetric Griess method [58].

3.3.5.2. Cytotoxicity. The release of cytoplasmic lactate dehydrogenase (LDH) is indicative of cell lysis. Macrophages were cultured and treated with spray dried microspheres as above, and at the end of incubation, the supernatants were collected. For maximum release, cells were cultured in 2% Triton X-100, and for spontaneous release, cells were cultured in medium alone. LDH activity was determined by a colorimetric commercial kit (from Doles), according to the manufacturer's instructions. The percentage of specific release was calculated as (test release − spontaneous release) / (maximum release − spontaneous release) × 100.

3.3.6. Preparation and characterization of composite microspheres as drug delivery systems: preliminary studies

3.3.6.1. Preparation. Chitosan microspheres were found to have great utility in drug carrier and delivery systems [24,47,48]. Preliminary studies were conducted in this work to evaluate the performance of the

chitosan–Aerosil R972 microspheres onto the drug release. Rifampicin was chosen as a model lipophilic drug to test the release behavior of the composite microspheres. Rifampicin is a class II drug of Biopharmaceutical Classification System (BCS), where rate and extent of dissolution are critical for optimum bioavailability [49]. The objective was to verify if the composite microspheres could delay the rifampicin release rate in simulated gastric fluid pH conditions. Experiments were performed following the same experimental procedure described for the production of the unloaded composite microspheres. Rifampicin (0.1 g) was added to the hydroalcoholic chitosan–silica dispersion before the high-pressure homogenization step.

3.3.6.2. Characterization. In U.S. Pharmacopeia (USP), 0.1 N HCl is an official dissolution medium to evaluate the in-vitro dissolution kinetics of rifampicin [50]. To carry out the in vitro release, a USP type II dissolution apparatus (paddle method) was used. Approximately 500 mg of rifampicin-loaded composite microspheres was dispersed in 900 ml of 0.1 M HCl (pH 1.2) maintained at 37 ± 1 °C under continuous stirring at 100 rpm for 2 h. The amount of drug introduced into the dissolution media assured the presence of sink conditions (maximum drug concentration $\ll C_{eq}$). At selected time intervals, 5 ml samples were withdrawn through a hypodermic syringe fitted with a 0.4 mm Millipore filter and assayed spectrophotometrically (Cintra 10E Spectrophotometer) at a wavelength of 334 nm, to evaluate the amounts of drug dissolved. Experiments were made in triplicate. The mean of five measurements was used to calculate the drug release from the drug-loaded composite microspheres for each batch.

Besides in-vitro drug release, X-ray powder diffraction, scanning electron (SEM) and laser diffraction granulometry were also used to characterize the rifampicin-loaded composite microspheres, using the experimental procedures already described in this paper for the unloaded composite microspheres.

3.3.7. Statistical analysis

All data were expressed as mean ± SEM, and for all analyses $P < 0.05$ was considered as significantly different.

4. Results and discussion

4.1. Contact angle of ethanol–water solutions on Aerosil R972

Wetting of different concentrations of water–ethanol solutions on Aerosil R972 pressed tablet surfaces is shown in Fig. 2. The transition between the two clearly defined states 'non-wetting' and 'wetting' could be identified from these experiments as shown in Fig. 2. This behavior is attributed to a decrease in surface tension with increasing ethanol concentration. The contact angle for ethanol–water solutions for Aerosil R972 was found to decrease with increasing ethanol concentration, and enters the 'wetting' region (Θ <90°) for an ethanol amount in the ethanol–water solutions higher than 17% w/w.

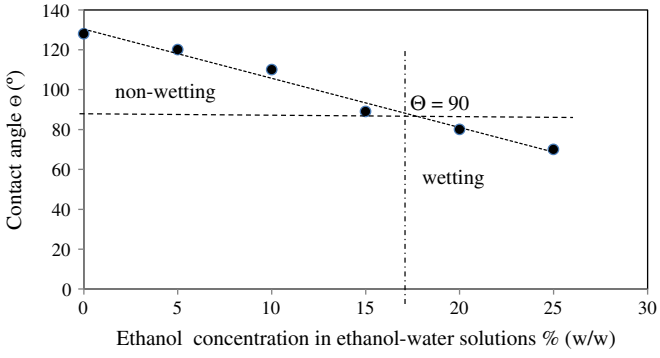

Fig. 2. Contact angle of ethanol–water solutions on Aerosil R972.

4.2. Physical characterization of composite microspheres

Chitosan and composite microspheres were characterized with respect to particle size, moisture content and superficial area. Table 1 summarizes the results.

Table 1 shows that in spite of the increase of the dispersion viscosity with the increase of Aerosil R972 concentration, only small variations in median diameter were observed for the different samples. There was no direct relationship between Aerosil R972 concentration and particle size, suggesting that the manufacturing method generated particles within a narrow size distribution regardless of silica concentration. The analysis of the particles distribution revealed that 90% of the particles were less than approximately 15 μm. Table 1 also shows that the specific surface area of composite microspheres increased with the Aerosil R972 content from 3.0 ± 0.2 $m^2\ g^{-1}$ (F1 sample) to 21.7 ± 0.7 $m^2\ g^{-1}$ (F4 sample), which could be expected considering the high specific surface area of the silica (110 ± 20 $m^2\ g^{-1}$). The residual water content ranged from 4.1 to 6.6% wt, increasing with the chitosan mass proportion.

Scanning Electron Microscopy (SEM) and Transmission Electron Microscopy (TEM) were used to examine the surface structure of the samples. In comparison, the SEM and TEM images of composite samples (F2, F3 and F4) suggested no variability of particle morphology with the Aerosil R972 concentration (data not shown). Representative SEM and TEM micrographs of F1 and F4 samples are shown in Figs. 3 and 4, respectively. As shown by these images, all spray dried powders consist of spherical structures.

Fig. 3D shows the visible nanosized silica particles on the F4 sample surfaces. From the TEM images (Fig. 4), it can be seen that these microspheres exhibited good transparency, indicating that silica nanoparticles did not aggregate, leading to the absence of phase separation in the polymeric matrix. Therefore, the chitosan–Aerosil R972 microspheres could be considered as nanocomposites consisting of homogeneously dispersed reinforcement (nanosized silica) within the chitosan matrix. From this reinforcement we could expect an influence on the mechanical and barrier properties of the composite microspheres.

To complete these data, the zeta potential of the spray dried microspheres and Aerosil R972 was measured as a function of pH and the results are shown in Fig. 5. It can be seen that the surface charges of the chitosan microspheres (F1) were positive in the range of pH 4.5 to 7.4. Due to its polymeric cationic characteristics, chitosan can interact with negatively charged Aerosil R972 also shown in Fig. 5. However, in spite of these probable electrostatic interactions, the surface charges of the composite microspheres were always positive even for F4, which are composite structures strongly charged in silica. This observation is of great importance, for example, when administering drugs by mucosal routes, since positive charge originating from chitosan microspheres is necessary for the interaction with negatively charged mucus, and consequently, mucoadhesion.

4.3. Thermal behavior

Thermogravimetric analysis (TG) and differential thermal analysis (DSC) were carried out under oxygen atmosphere to determine the inorganic content of the composite microspheres and to investigate their thermal stability. Table 2 summarizes the thermal parameters.

The inorganic content remaining after complete thermal degradation of the organic material at 800 °C is shown in Table 2. It ranged from 21% to 58% into the chitosan microspheres loaded with Aerosil R972. Fig. 6 shows the TG curves of the spray dried microspheres with different Aerosil R972 loadings, in comparison to microspheres containing neat chitosan. It can be seen that (neat) chitosan microspheres underwent a single stage of degradation in the range 198–243 °C (T_{peak} at 226 °C). All experiments were conducted in oxidative

Table 1
Physical properties of chitosan–Aerosil R972 microspheres.

Code	Chitosan: Aerosil R972 (theoretical mass proportion)	Suspension viscosity at 25 °C (cp)	Water content % (w/w)	Specific surface area ($m^2\ g^{-1}$)	$D_{(4.3)}$ (μm)	$D_{(0.1)}$ (μm)	$D_{(0.9)}$ (μm)	Span
F1	1:0	20.4 ± 0.1	6.2 ± 0.9	3.0 ± 0.2	5.1 ± 0.1	1.9 ± 0.1	17.5 ± 2.1	2.4
F2	10:1	28.2 ± 0.2	6.6 ± 0.1	4.1 ± 0.3	6.6 ± 0.5	0.9 ± 0.1	15.3 ± 0.5	2.4
F3	2:1	37.1 ± 0.3	5.3 ± 0.1	8.8 ± 0.3	7.9 ± 0.1	2.6 ± 0.1	14.1 ± 0.6	1.7
F4	1:1	60.5 ± 0.5	4.1 ± 0.1	21.7 ± 0.7	5.9 ± 0.1	2.1 ± 0.1	10.5 ± 0.5	1.6

atmosphere. However, according to the literature, the main difference in thermal degradation of chitosan in non-oxidative (nitrogen purge) and in oxidative atmospheres occurs above 400 °C [46], where strong exothermic effects can be observed in the presence of oxygen indicating that an efficient oxidation followed by further decomposition of oxidized chitosan takes place. The degradation mechanism is very complex including the dehydration, deacetylation and chain scission [51], but its understanding is out of the aims of this study.

The main findings from these analysis are the remarkable shift of the temperature of decomposition to higher values which appeared for the chitosan microspheres containing 21.5% (F2) and 39.9% w/w of Aerosil R972 (F3), as shown in Fig. 6 and given in Table 2. This is an indication that the addition of Aerosil R972 nanosized particles promotes chitosan stabilization against oxidative degradation. In summary, when the results of neat chitosan microspheres are compared to the results of chitosan–Aerosil R972 microspheres in terms of thermal behavior, there are many important differences which might be due to the interaction between chitosan and Aerosil R972.

To get more insight on the thermal behavior of the spray dried composite microspheres, DSC measurements were performed and the results are shown in Fig. 7. The DSC thermograms show broad endothermic peaks over a large temperature range (<100 °C), which is attributed to water loss due to evaporation of absorbed water. The main event of these calorimetric curves is an exothermic peak centered around 250–310 °C in Fig. 7 for chitosan (F1) and composite (F2, F3 and F4) microspheres, owing to the thermal degradation of the microspheres. The peak of pure chitosan is read at 251 °C. With the addition of Aerosil R972, this exothermic peak shifted to the high temperature region (288–309 °C). This behavior confirms the results already shown by TGA analysis that Aerosil R972 in appropriate content increased the thermal stability of the chitosan microspheres.

4.4. Structural characterization

4.4.1. X-ray diffraction

The XRD technique is based on the elastic scattering of X-rays from structures that have long-range order. It is an efficient analytical technique to identify and characterize crystalline materials. The X-ray diffraction patterns (Fig. 8) show that Aerosil R972 nanoparticles, spray dried neat chitosan microspheres and composite microspheres

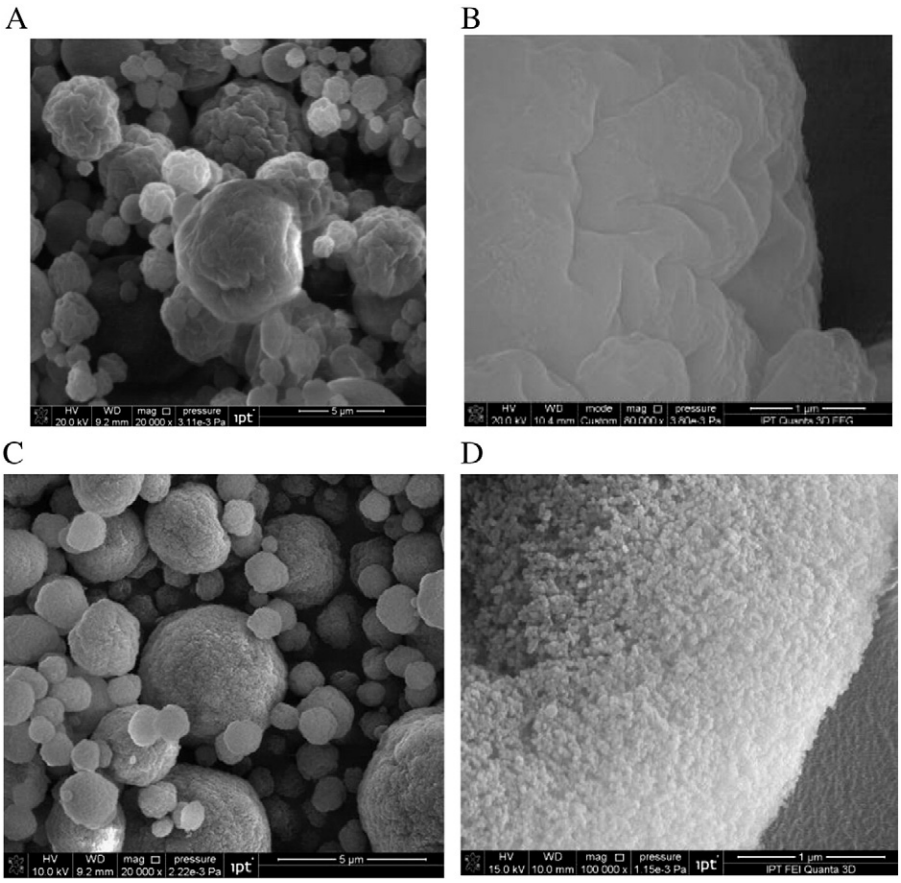

Fig. 3. SEM images of the composite microspheres. (A) and (B) F1 (neat chitosan); (C) and (D) F4 (58.1% Aerosil R972 loading).

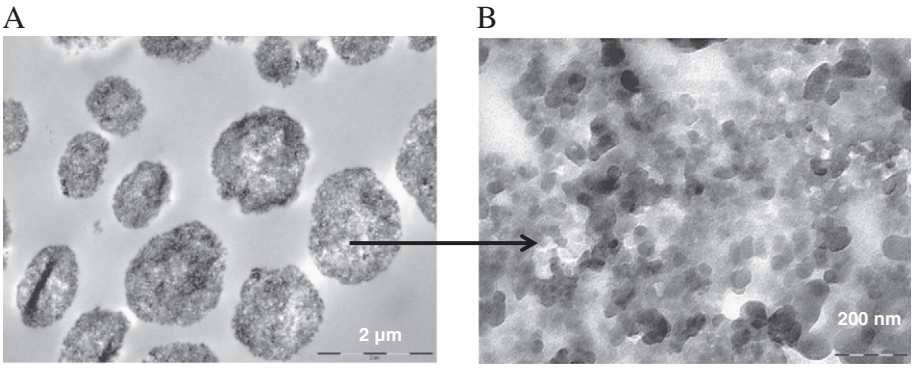

Fig. 4. TEM images of the composite microspheres. (A) and (B) F4 (58.1% Aerosil R972 loading).

can be identified as amorphous, due to the broad diffraction halo they exhibited.

4.4.2. FT-IR spectroscopy

The bonding structure of the composite microspheres was further investigated by FTIR spectroscopy. The FTIR spectra of F2, F3 and F4 samples (Fig. 9) present the characteristic peaks of chitosan and Aerosil R972.

The spectra of unmodified chitosan microspheres (Fig. 9a) showed a broad absorption band at 3444 cm^{-1} attributed to the stretching vibrations of OH groups, which are overlapped to the stretching vibration of N – H. The characteristic absorption of chitosan is the band at 1595 cm^{-1}, which is assigned to the stretching vibration of amino group of chitosan and 1325 cm^{-1} assigned to vibration of C – H. The peak at 1085 cm^{-1} indicates C – O stretching vibration [52,53]. The peaks around 895 and 1155 cm^{-1} correspond to stretching vibrations of C – O – C groups in saccharide structure of chitosan [54,55].

The FTIR spectra of Aerosil R972 (Fig. 9e) showed an absorption peak at about 1109 cm^{-1}, attributed to the asymmetric stretching vibrations of the Si – O – Si bonds of silica oxide, while the peak at 810 cm^{-1} can be attributed to the symmetric deformation of the Si – O – Si bonds. These are typical absorption bands for Si – O – Si network vibrations [56].

The IR spectra of composite microspheres show the characteristic bands of both chitosan and Aerosil R972 (Fig. 9b to d). They are of similar shape; however, several characteristic bands are shifted, deformed or disappeared, especially in the region between 1000 and 1400 cm^{-1}.

Also for chitosan, the absorption band of amide II (1595 cm^{-1}) is shifted a little for the short wave (1560 cm^{-1}) and the characteristic bands in chitosan skeleton at 1032, 1155, 1032 and 895 cm^{-1} are observed with slight intensity or disappeared (see Fig. 9d). This evidences that the groups of these bands have taken part in bonding with Aerosil R972.

4.5. Moisture sorption characteristics

The objective here was to verify the effects of Aerosil R972 on the barrier properties of chitosan against high humidity. The equilibrium moisture sorption isotherms (first sorption cycle) for each of the samples are plotted in Fig. 10. Although two cycles were conducted for each material, moisture desorption from the first cycle was reversible. Subsequently, such data were omitted for better clarity between samples.

The results suggest that the affinity of composite microspheres for moisture sorption decreased, compared to neat chitosan microspheres. To further investigate the relationship between moisture sorption and the relative concentration of silica in the composite microspheres, the equilibrium mass content of each sample at high relative humidity (70% RH used as a percentage of reference) was plotted against Aerosil R972 concentration (Fig. 11). The analysis in Fig. 11 also suggested a direct linear relationship between moisture sorption at 70% RH and Aerosil R972 concentration ($R^2 = 0.9986$), with increased silica content resulting in a decreased affinity for moisture sorption.

4.6. Acid stability

Chitosan is soluble in acidic pH, therefore, the purpose of carrying out this study that we called 'acid stability experiment' was to measure the effect of silica on the solubility of composite microspheres in acidic

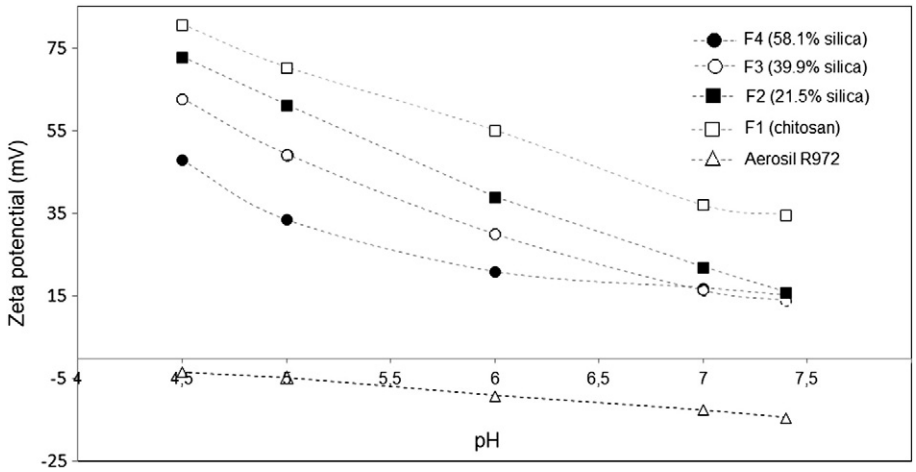

Fig. 5. Zeta potential of composite microspheres and neat Aerosil R972 as a function of pH.

Table 2
Thermal parameters obtained from thermogravimetric analysis of chitosan in oxygen temperature.

Code	Chitosan: Aerosil R972 (theoretical mass proportion)	Inorganic loading % (w/w)[a]	Chitosan decomposition temperature	
			T_{onset} (°C)	T_{peak} (°C)
F1	1:0	0	198	226
F2	10:1	21.5 ± 0.3	217	248
F3	2:1	39.9 ± 0.4	251	282
F4	1:1	58.1 ± 0.7	252	285

[a] Ash remaining after complete degradation of samples at 800 °C.

medium. The light transmission data in Table 3 are presented as percentages. The 0.1 N HCl is the sample providing 100% transmission.

Chitosan microspheres dissolved in the acidic medium leading to a medium more transparent (92% transmission). However, if the particles do not dissolve, the light transmission through the medium decreases. Since the decrease in turbidity is directly dependent on the dissolution of the microspheres, transmission is a measure of the concentration of non-dissolved microspheres. To sum up, a low transmission indicates high stability of microspheres in the acidic medium (low or slow dissolution rate), and a high transmission implies that the microspheres dissolved in HCl.

It can be observed in Table 3 that increasing Aerosil R972 loadings reduced % light transmission through the suspensions, suggesting that microspheres dissolved more slowly. Presumably, this "acid-stability" arises by virtue of coating the surface of the microsphere with non-acid-labile silica, thereby preventing contact between the acid and the chitosan, which would otherwise dissolve.

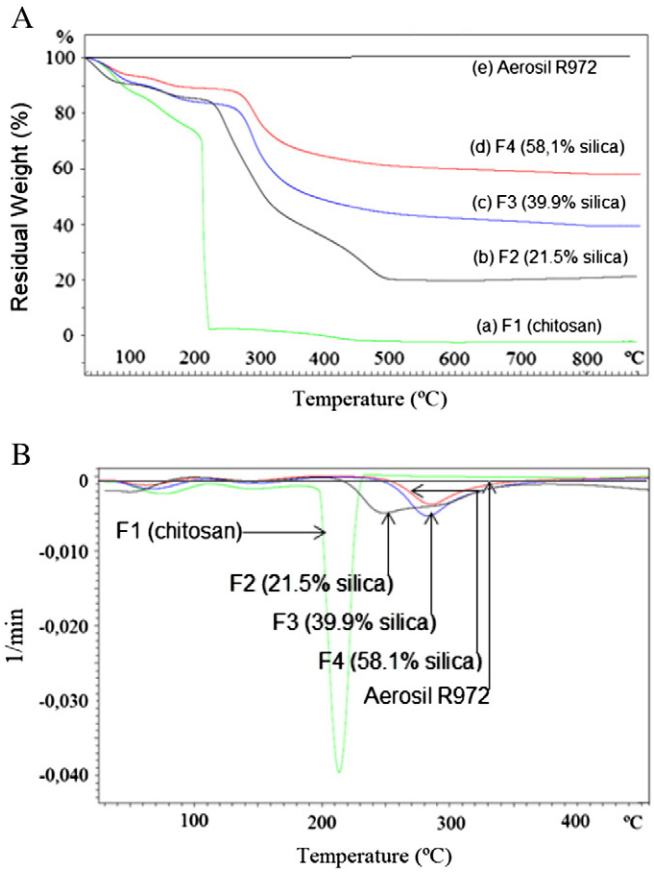

Fig. 6. TGA thermograms (A) and derivative mass loss (DTG) (B) versus temperature, with heating rate of 10 °C min^{-1} for composite microspheres with different Aerosil R972 loadings: (a) F1 (neat chitosan), (b) F2 (21.5%), (c) F3 (39.9%), (d) F4 (58.1%), and (e) neat Aerosil R972.

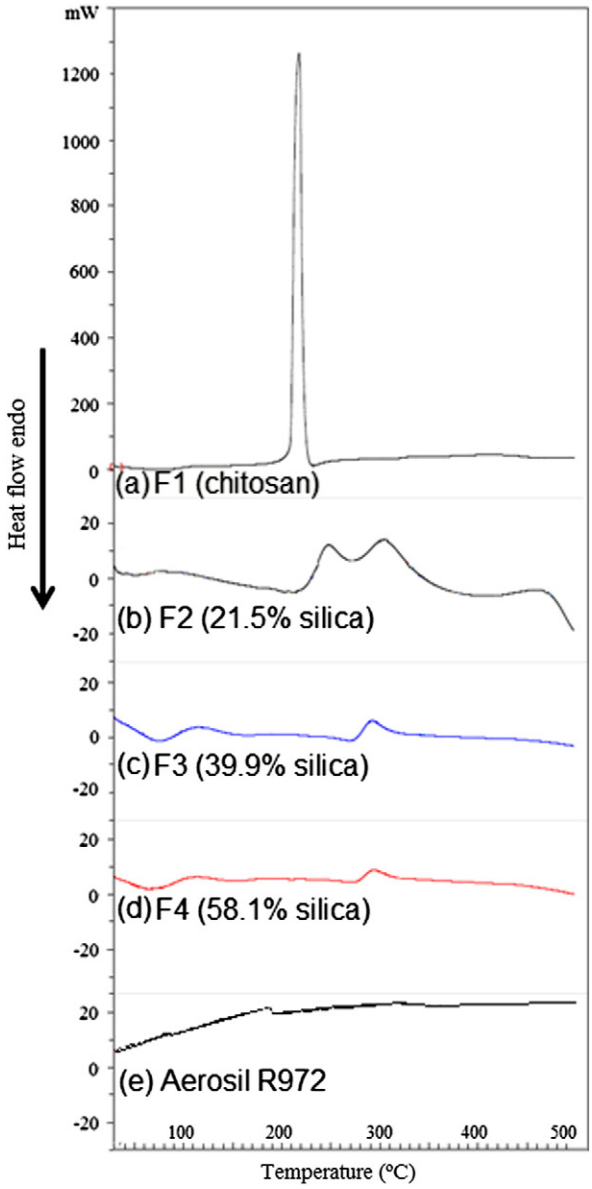

Fig. 7. DSC thermograms for composite microspheres with different Aerosil R972 loadings: (a) F1 (neat chitosan), (b) F2 (21.5%), (c) F3 (39.9%), (d) F4 (58.1%), and (e) neat Aerosil R972.

4.7. Biological assays

The composite microspheres with the highest Aerosil R972 loading (F4) were chosen for biological assays due to their properties (better chemical resistance in acidic medium, reduced moisture affinity). Their capacity to activate macrophages to produce nitric oxide was tested as an indication of pro-inflammatory potential. Microspheres containing only chitosan (F1 sample) were also tested as control.

Fig. 12 shows that concentrations of either particles as high as 1000 μg ml^{-1} did not stimulate macrophages to produce nitric oxide, compatible with a low pro-inflammatory action. The capacity of F1 and F4 microspheres to induce cytotoxicity was evaluated by their capacity to induce cytoplasmic LDH leakage from macrophages. Fig. 13 shows that despite their similar concentrations necessary to produce 50% of cell lysis (IC50, 220 μg ml^{-1} and 237 μg ml^{-1}, respectively), at concentrations lower than 100 μg ml^{-1}, F4 is less ($P < 0.05$) cytotoxic than F1. Together, these results indicate that F1 and F4 microspheres are not prone to induce inflammation, and that coating with 58% Aerosil

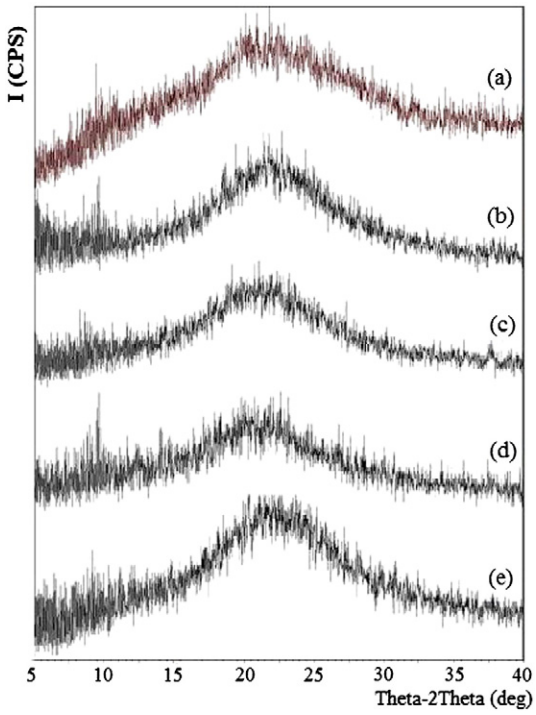

Fig. 8. DRX diffractograms for composite microspheres with different Aerosil R972 loadings: (a) F1 (neat chitosan), (b) F2 (21.5%), (c) F3 (39.9%), (d) F4 (58.1%), and (e) neat Aerosil R972.

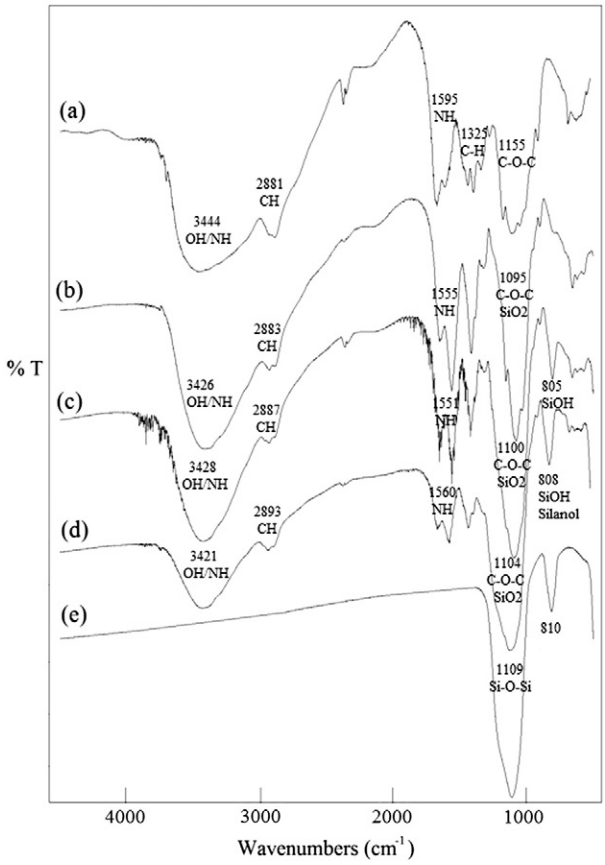

Fig. 9. FTIR spectra for composite microspheres with different Aerosil R972 loadings: (a) F1 (neat chitosan), (b) F2 (21.5%), (c) F3 (39.9%), (d) F4 (58.1%), and (e) neat Aerosil R972.

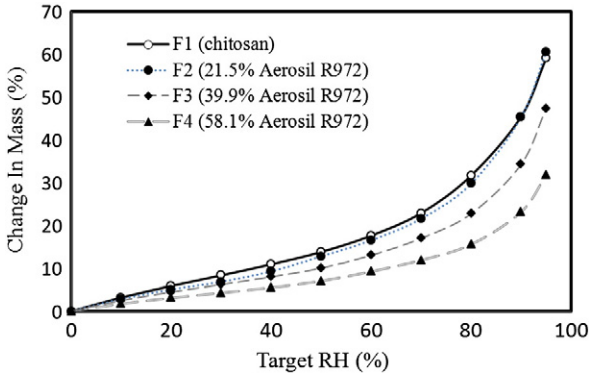

Fig. 10. DVS sorption isotherms for spray dried composite microspheres with varying percentages of Aerosil R972.

R972 as in F4 rendered chitosan microspheres more biocompatible. This effect is possibly due to a stealth effect of hydrophobic silica preventing strong electrostatic interaction of cationic chitosan with the negatively charged cell membrane and cytosol leakage.

4.8. Composite microspheres as drug delivery systems: preliminary studies

Consistently with our attempt, a synergistic effect of chitosan and Aerosil R972 as well as some possible interfacial interactions between them via electrostatic interactions and H-bonds could change properties of the spray dried composite microspheres such as thermal degradation, moisture affinity and acid stability. Preliminary studies were conducted to evaluate the performance of the composite microspheres onto the drug release at acidic conditions, using rifampicin as model drug.

The formulation of choice was F4 (58.1% Aerosil R972) due to its best performance to control chitosan dissolution in acidic medium demonstrated from the acid stability experiments. F1 was used as control (neat chitosan). The new formulations were named rifampicin-loaded F1 and rifampicin-loaded F4, respectively.

Fig. 14 presents the SEM images of raw rifampicin and the rifampicin-loaded F4 microspheres. The raw rifampicin had an irregular shape and broad particle size distribution ranging from 39 to 603 μm (particle size distribution determined by laser diffraction analysis, data not shown). Evidently, the particle size of the spray dried rifampicin is

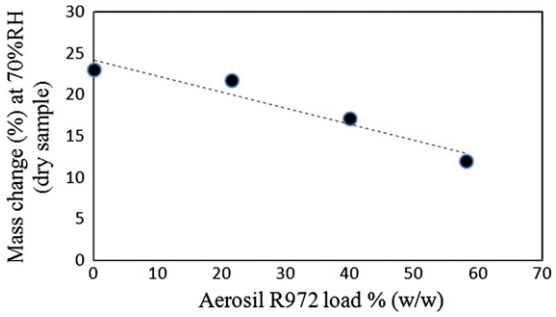

Fig. 11. Mean moisture sorption at 70% RH plotted as a function of Aerosil R972 concentration.

Table 3
Acid stability of chitosan–Aerosil R972 microspheres.

Code	Chitosan: Aerosil R972 (theoretical mass proportion)	Inorganic loading % (w/w)	% light transmission
F1	1:0	0	92.1 ± 0.3
F2	10:1	21.5 ± 0.3	72.9 ± 0.4
F3	2:1	39.9 ± 0.4	30.0 ± 0.8
F4	1:1	58.1 ± 0.7	10.6 ± 2.8

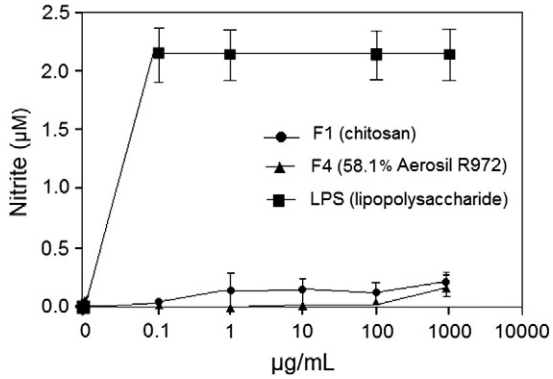

Fig. 12. Lack of stimulation of nitric oxide production by macrophages. Mouse peritoneal macrophages (5×10^5) were cultured at 37 °C for 48 h in 200 μl of medium containing varying concentrations of F1 and F4, as indicated. The supernatants were collected, and the nitrite concentration was colorimetrically determined using the Griess method. Positive controls were cells cultured with 1 μg ml^{-1} of lipopolysaccharide (LPS, OD = 2.05). Negative controls were cells in medium with 1% DMSO (OD = 0.43). Means ± SD, n = 3. Representative of 2 different experiments using different batches of samples.

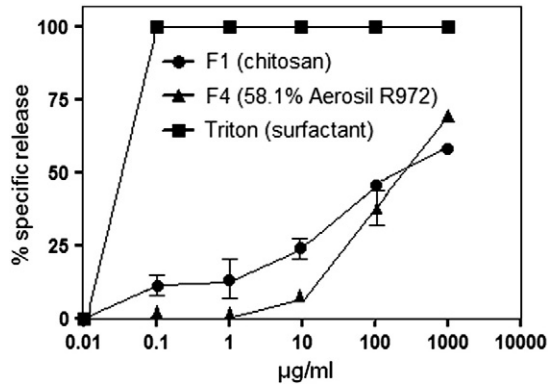

Fig. 13. Cytotoxicity to macrophages: mouse peritoneal macrophages were incubated for 48 h in the presence of varying concentrations of F1 and F4 as indicated. At the end of incubation time the cell supernatants were collected for colorimetric measurement of the released lactate dehydrogenase. For maximum (100%) release, cells were cultured with 2% Triton X-100 (OD = 1.36). For spontaneous release, cells were cultured in medium with 1% DMSO (OD = 0.14). Means ± SD, n = 3. *$P < 0.05$ in relation to F4. Representative of two different experiments using different batches of samples.

significantly smaller and more uniform than that of the raw drug. Rifampicin-loaded F4 sample exhibited regular spherical structure and particle size close to those of the unloaded composite microspheres (ranging from 2 to 12 μm, data measured by laser diffraction analysis, not shown).

X-ray diffraction analysis confirmed that formulation process altered the crystalline nature of rifampicin. The corresponding X-ray diffraction patterns were displayed in Fig. 15. It can be seen that the raw rifampicin

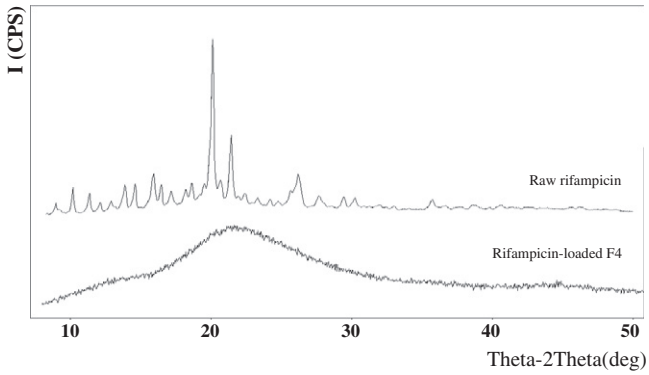

Fig. 15. DRX diffractograms for: raw rifampicin and rifampicin-loaded composite microspheres (rifampicin-loaded F4).

exhibited intense crystalline peaks between 10° and 30°. However, a broad and diffuse maxima peak at 22° was detected in the pattern of rifampicin-loaded F4 microspheres, demonstrating the reduced crystalline nature of the powder.

The in vitro release profiles are compared in Fig. 16. Firstly, this figure shows that raw rifampicin dissolved more slowly than spray-dried rifampicin, due to a higher surface area (smaller particles) and lower degree of crystallinity. It is known that transforming the physical state of the drug (crystalline to amorphous) would lead to a high-energy state and high disorder, resulting in enhanced dissolution rate [57]. Secondly, rifampicin-loaded F1 microspheres (neat chitosan) did not delay the dissolution of the drug in the acidic medium, the dissolution was even to close to that of the control (immediate release). In turn, the results of the dissolution kinetics of rifampicin-loaded F4 microspheres showed significantly ($P < 0.05$) reduced percentage drug release compared to rifampicin-loaded F1 microspheres.

The present study aimed at testing a protector effect of the composite microsphere membrane against rifampicin dissolution in acidic medium. The drug release could be extended under acidic condition within the first 30 min when rifampicin was loaded in rifampicin-loaded F4 microspheres.

5. Conclusions

In this study we proposed to develop spray-dried microspheres composed of chitosan and hydrophobic silica particles aiming at increased thermal and acidic stabilities, as well as improved drug release properties in acidic medium.

Loading the chitosan microspheres with up to 58% Aerosil R972 did not alter significantly their average particle size, however the specific surface area was increased. Increasing the Aerosil R972 content led to increased thermal and acid stability, and also lower moisture affinity.

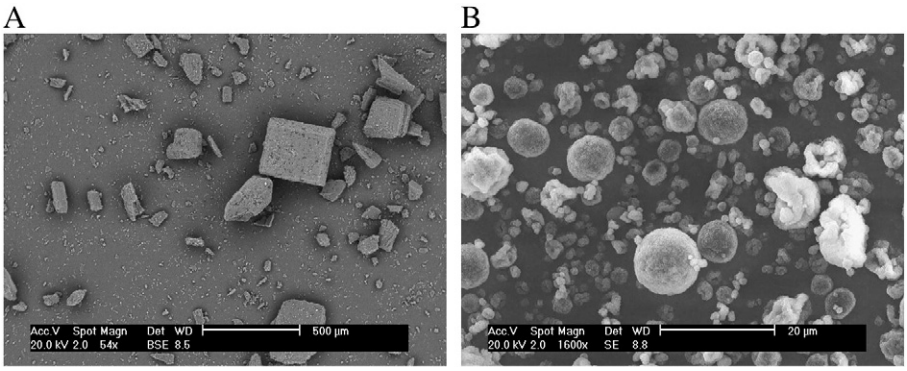

Fig. 14. SEM images of: (A) raw rifampicin, (B) rifampicin-loaded composite microspheres (rifampicin-loaded F4).

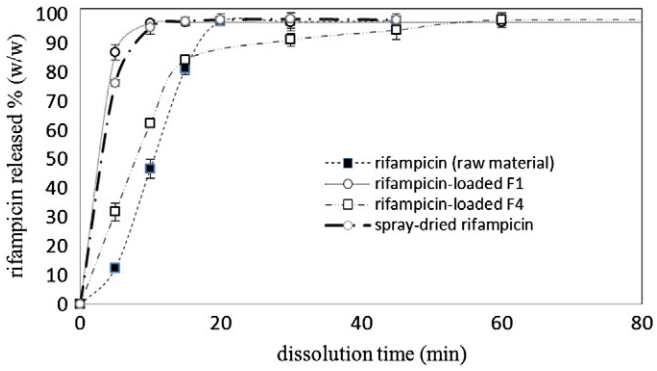

Fig. 16. Dissolution kinetics for rifampicin-loaded microspheres (37 °C, dissolution medium 0.1 N HCl pH 1.2).

The improved properties were attributed to some interaction likely through hydrogen bonds between hydrophobic (Aerosil R972) and hydrophilic components (chitosan), which were confirmed by the structural characterization studies.

In vitro studies indicated low cytotoxicity and low capacity to activate cell production of the pro-inflammatory mediator nitric oxide. Together these findings encourage further exploration of our chitosan–hydrophobic silica microspheres as novel oral or mucosal drug delivery systems.

Acknowledgments

Brazilian Research Councils (CNPq, Council for Scientific and Technological Development and CAPES, Higher Education Research Council) are acknowledged for fundings. We would like to thank IPT (Institute for Technological Research of Sao Paulo State, Brazil) for their technical support.

References

[1] M.N.V. Ravi Kumar, A review of chitin and chitosan applications, React. Funct. Polym. 46 (1) (2000) 1–27.
[2] T.A. Sonia, C.P. Sharma, Chitosan and its derivatives for drug delivery perspective, Adv. Polym. Sci. 243 (2011) 23–53.
[3] J. Bergera, M. Reista, J.M. Mayera, O. Feltb, N.A. Peppasc, R. Gurny, Structure and interactions in covalently and ionically crosslinked chitosan hydrogels for biomedical applications, Eur. J. Pharm. Biopharm. 57 (1) (2004) 19–34.
[4] M. Dasha, F. Chiellinia, R.M. Ottenbriteb, E. Chiellini, Chitosan - a versatile semi-synthetic polymer in biomedical applications, Prog. Polym. Sci. 36 (8) (2011) 981–1014 (619).
[5] N.M. Alves, J.F. Mano, Chitosan derivatives obtained by chemical modifications for biomedical and environmental applications, Int. J. Biol. Macromol. 43 (5) (2008) 401–414.
[6] F. Devlieghere, A. Vermeulen, J. Debevere, Chitosan: antimicrobial activity, interactions with food components and applicability as a coating on fruit and vegetables, Food Microbiol. 21 (6) (2004) 703–714.
[7] P.K. Dutta, S. Tripathi, G.K. Mehrotra, J. Dutta, Perspectives for chitosan based antimicrobial films in food applications, Food Chem. 114 (2009) 1173–1182.
[8] F. Shahidi, J.K.V. Arachchi, Y.J. Jeon, Food applications of chitin and chitosans, Trends Food Sci. Technol. 10 (1999) 37–51.
[9] E. Onsoyen, O. Skaugrud, Metal recovery using chitosan, J. Chem. Technol. Biotechnol. 49 (1990) 395–404.
[10] D. Zenga, J. Wu, J.F. Kennedy, Application of a chitosan flocculant to water treatment, Carbohydr. Polym. 71 (2008) 135–139.
[11] R. Divakaran, V.N.S. Pillai, Flocculation of kaolinite suspensions in water by chitosan, Water Res. 35 (2001) 3904–3908.
[12] M.G. Peter, Applications and environmental aspects of chitin and chitosan, J. Macromol. Sci. A: Pure Appl. Chem. 32 (4) (1995) 629–640.
[13] M. Zhang, T. Tan, H. Yuan, C. Rui, Insecticidal and fungicidal activities of chitosan and oligo-chitosan, J. Bioact. Compat. Polym. 18 (2003) 391–400.
[14] D.W. Lee, H. Lim, H.N. Chong, W.S. Shim, Advances in chitosan material and its hybrid derivatives: a review, Open Biomater. J. 1 (2009) 10–20.
[15] S.A. Agnihotri, N.N. Mallikarjuna, T.M. Aminabhavi, Recent advances on chitosan-based micro- and nanoparticles in drug delivery, J. Control. Release 100 (2004) 5–28.
[16] S. Gordon, E. Teichmann, K. Young, K. Finnie, T. Rades, S. Hook, In vitro and in vivo investigation of thermosensitive chitosan hydrogels containing silica nanoparticles for vaccine delivery, Eur. J. Pharm. Sci. 41 (2010) 360–368.
[17] V. Bansal, P.K. Sharma, N. Sharma, O.P. Prakash, R. Malviya, Applications of chitosan and chitosan derivatives in drug delivery, Adv. Biol. Res. 5 (2011) 28–37.
[18] E. Gavini, G. Rassu, C. Muzzarelli, M. Cossu, P. Giunchedi, Spray-dried microspheres based on methylpyrrolidinone chitosan as new carrier for nasal administration of metoclopramide, Eur. J. Pharm. Biopharm. 68 (2008) 245–252.
[19] U.K. Parida, A.K. Nayak, B.K. Binhani, P.L. Nayak, Synthesis and characterization of chitosan-polyvinyl alcohol blended with cloisite 30B for controlled release of the anticancer drug curcumin, J. Biomater. Nanobiotechnol. 2 (2011) 414–425.
[20] X. Wang, Y. Du, J. Luo, B. Lin, J.F. Kennedy, Chitosan/organic rectorite nanocomposite films: structure, characteristic and drug delivery behavior, Carbohydr. Polym. 69 (2007) 41–49.
[21] C. Chen, Z. Gao, X. Qiu, S. Hu, Enhancement of the controlled-release properties of chitosan membranes by crosslinking with suberoyl chloride, Molecules 18 (2013) 7239–7252.
[22] K.C. Gupta, F.H. Jabrail, Glutaraldehyde cross-linked chitosan microspheres for controlled release of centchroman, Carbohydr. Res. 342 (2007) 2244–2252.
[23] S. Ramachandran, G. Thirumurugan, M.D. Dhanaraju, Development and evaluation of biodegradable chitosan microspheres loaded with ranitidine and cross linked with glutaraldehyde, Am. J. Drug Discov. Dev. 1 (2011) 105–120.
[24] E.B. Mirzaei, S.A.A. Ramazani, M. Shafiee, M. Danaei, Studies on glutaraldehyde crosslinked chitosan hydrogel properties for drug delivery systems, Int. J. Polym. Mater. Polym. Biomater. 62 (2013) 605–611.
[25] W.L. Du, S.S. Niu, Z.R. Xu, Y.L.Xu. Preparation, Characterization, and adsorption properties of chitosan microspheres crosslinked by formaldehyde for copper (ii) from aqueous solution, J. Appl. Polym. Sci. 111 (2009) 2881–2885.
[26] A. Singh, S.S. Narvi, P.K. Dutta, N.D. Pandey, External stimuli response on a novel chitosan hydrogel crosslinked with formaldehyde, Bull. Mater. Sci. 29 (2006) 233–238.
[27] Q. Yang, F. Dou, B. Liang, Q. Shen, Studies of cross-linking reaction on chitosan fiber with glyoxal, Carbohydr. Polym. 59 (2005) 205–210.
[28] M. Moniera, D.M. Ayad, Y. Wei, A.A. Sarhan, Preparation of cross-linked chitosan/glyoxal molecularly imprinted resin for efficient chiral resolution of aspartic acid isomers, Biochem. Eng. J. 51 (2010) 140–146.
[29] T.C. Coelho, R. Lausa, A.S. Mangrich, V.T. de Fávere, M.C.M. Laranjeira, Effect of heparin coating on epichlorohydrin cross-linked chitosan microspheres on the adsorption of copper (II) ions, React. Funct. Polym. 67 (2007) 468–475.
[30] M. Sahin, N. Kocak, G. Arslan, H.I. Ucan, Synthesis of crosslinked chitosan with epichlorohydrin possessing two novel polymeric ligands and its use in metal removal, J. Inorg. Organomet. Polym. Mater. 21 (2011) 69–80.
[31] R. Harris, E. Lecumberri, A. Heras, Chitosan–genipin microspheres for the controlled release of drugs: clarithromycin, tramadol and heparin, Mar. Drugs 8 (2010) 1750–1762.
[32] F.L. Mi, H.W. Sung, S.S. Shyu, Synthesis and characterization of a novel chitosan-based network prepared using naturally occurring crosslinker, J. Polym. Sci. A Polym. Chem. 38 (15) (2000) 2804–2814.
[33] B.F. Oliveira, M.H.A. Santana, M.I. Ré, Spray-dried chitosan microspheres cross-linked with d, l-glyceraldehyde as a potential drug delivery system: Preparation and characterization, Braz. J. Chem. Eng. 22 (2005) 353–360.
[34] B.F. Oliveira, M.H.A. Santana, M.I. Ré, Spray-dried chitosan microspheres as a pDNA Carrier, Dry. Technol. 24 (2006) 373–382.
[35] S. Hua, H. Yang, A. Wang, A pH-sensitive nanocomposite microsphere based on chitosan and montmorillonite with in vitro reduction of the burst release effect, Drug Dev. Ind. Pharm. 36 (9) (2010) 1106–1114.
[36] S.F. Wang, L. Shen, Y.J. Tong, L. Chen, I.Y. Phang, P.Q. Lim, T.X. Li, Biopolymer chitosan/montmorillonite nanocomposites: preparation and characterization, Polym. Degrad. Stab. 90 (2005) 123–131.
[37] I. Salcedo, C. Aguzzi, G. Sandri, M.C. Bonferoni, M. Mori, P. Cerezo, R. Sáncheza, C. Viserasa, C. Caramella, In vitro biocompatibility and mucoadhesion of montmorillonite chitosan nanocomposite: A new drug delivery, Appl. Clay Sci. 55 (2012) 131–137.
[38] J.H. An, S. Dulz, Adsorption of tannic acid on chitosan–montmorillonite as a function of pH and surface charge properties, Appl. Clay Sci. 36 (2007) 256–264.
[39] K.H. Liu, T.Y. Liu, S.Y. Chen, D.M. Liu, Effect of clay content on electrostimulus deformation and volume recovery behavior of a clay–chitosan hybrid composite, Acta Biomater. 3 (2007) 919–926.
[40] W. Khunawattanakul, S. Puttipipatkhachorn, T. Rades, T. Pongjanyakul, Novel chitosan magnesium aluminum silicate nanocomposite film coatings for modified-release tablets, Int. J. Pharm. 407 (2011) 132–141.
[41] K. Chrissafis, K.M. Paraskevopoulos, G.Z. Papageorgiou, D.N. Bikiaris, Thermal and dynamic mechanical behavior of bionanocomposites: fumed silica nanoparticles dispersed in poly(vinyl pyrrolidone), chitosan, and poly(vinyl alcohol), J. Appl. Polym. Sci. 110 (2008) 1739–1749.
[42] M.R. Gandhi, S. Meenakshi, Preparation and characterization of La(III) encapsulated silica gel/chitosan composite and its metal uptake studies, J. Hazard. Mater. 203–204 (2012) 29–37.
[43] T. Witoon, M. Chareonpanich, J. Limtrakul, Effect of acidity on the formation of silica–chitosan hybrid materials and thermal conductive property, J. Sol-Gel Sci. Technol. 51 (2) (2009) 146–152.
[44] A. Berthold, K. Cremer, J. Kreuter, Influence of crosslinking on the acid stability and physicochemical properties of chitosan microspheres, STP Pharm. Sci. 6 (1996) 358–364.
[45] S. Dhawan, K. Dhawan, M. Varma, V.R. Sinha, Application of poly (ethylene oxide) in drug delivery systems, Pharm. Technol. 29 (5) (2005) 72–79.
[46] J. Zawadzki, H. Kaczmarek, Thermal treatment of chitosan in various conditions, Carbohydr. Polym. 80 (2) (2010) 394–400.
[47] M.S. Kamble, O.R. Mane, S.S. Mane, V.G. Borwandkar, P.D. Chaudhari, Formulation & characterisation of chitosan based microspheres of salbutamol sulphate dry powder inhaler formulation, J. Drug Deliv. Ther. 2 (5) (2012) 37–41.

[48] V. Tokárová, O. Kašpar, Z. Knejzlík, P. Ulbrich, Fr. Štěpánek, Development of spray-dried chitosan microcarriers for nanoparticle delivery, Powder Technol. 235 (2013) 797–805.
[49] A. Viçosa, J.J. Letourneau, F. Espitalier, M.I. Ré, An innovative antisolvent precipitation process as a promising technique to prepare ultrafine rifampicin particles, J. Cryst. Growth 342 (2012) 80–87.
[50] S.Q. Henwood, M.M. de Villiers, W. Liebenberg, A.P. Lötter, Solubility and dissolution properties of generic rifampicin raw materials, Drug Dev. Ind. Pharm. 26 (4) (2000) 403–408.
[51] T.-M. Don, C.-Y. Chuang, W.-Y. Chiu, Studies on the degradation behavior of chitosan-g-poly(acrylic acid) copolymers, Tamkang J. Sci. Eng. 5 (4) (2002) 235–240.
[52] E.S. Costa-Júnior, M.M. Pereira, H.S. Mansur, Properties and biocompatibility of chitosan films modified by blending with PVA and chemically crosslinked, J. Mater. Sci. Mater. Med. 20 (2009) 553–561.
[53] K.S.V. Krishna Rao, B. Vijaya Kumar Naidu, M.C.S. Subha, M. Sairam, T.M. Aminabhavi, Novel chitosan-based pH-sensitive interpenetrating network microgels for the controlled release of cefadroxil, Carbohydr. Polym. 66 (2006) 333–344.
[54] M. Miya, R. Iwamoto, S. Yoshikawa, S. Mima, I.R. spectroscopic determination of CONH content in highly deacylated chitosan, Int. J. Biol. Macromol. 2 (1980) 323.
[55] C. Radhakumary, G. Divya, P.D. Naira, S. Mathew, C.P. Reghunadhan Nair, Graft Copolymerization of 2-Hydroxy Ethyl Methacrylate onto Chitosan with Cerium (IV) Ion. I. Synthesis and Characterization, J. Macromol. Sci. A: Pure Appl. Chem. 40 (2003) 715–730.
[56] A.G.S. Prado, E.A. Faria, P.M. Padilha, Aplicação e modificação química da sílica gel obtida de areia, Quim. Nova 28 (3) (2005) 544–547.
[57] G. Van den Mooter, The use of amorphous solid dispersions: a formulation strategy to overcome poor solubility and dissolution rate, Drug Discov. Today: Technol. 9 (2012) 79–85.
[58] L.C. Green, D.A. Wagner, J. Glogowski, P.L. Skipper, J.S. Wishnok, S.R. Tannenbaum, Analysis of nitrate, nitrite, and [15 N] nitrate in biological fluids, Anal. Biochem. 126 (1982) 131–138.